

1

2

3

4

Supplemental Materials

6

Regeneration Alters Open Chromatin and *Cis*-Regulatory Landscape of Erythroid Precursors

5

11 File Contains:

12 Supplemental Methods

13 Supplemental Figures and Figure Legends

14 Supplemental References

15

16

17

18

19

20 **Supplemental Methods**

21

22 **ATAC-seq Data Analysis**

23 To analyze acute and long-lasting peaks, we used MEME-ChIP. Differential ATAC-seq peaks
24 were called using Manorm (1,2). Acute peaks were defined as differential between Day 0 and
25 Day 7 but resolved by Day 35. Long-lasting peaks were peaks that were differential between
26 Day 0 and Day 7 and remained changed by Day 35. To compare PHZ-induced changes with
27 ATAC-seq changes that occur during haematopoiesis we downloaded the publicly available
28 data at the GEO accession GSE59992. The fastq files were downloaded and remapped to
29 mm10 using bowtie2 (3). Samtools was used to quality filter (q=10) and sort reads (4). PCR
30 duplicates were removed with picard MarkDuplicates (5). Finally biological replicates were
31 merged, and bigwig files were generated using deeptools bamCoverage –normalizeUsing
32 BPM (6). Log2 fold changes in signal between CMP and MEP as well as between MEP and
33 ErA were then calculated for loci corresponding to all differential peaks found in PHZ
34 timepoints. Pearson correlation was then used to compare these changes to that of day 7 vs
35 day 0 PHZ for these loci.

36

37

38

39

40

41

42

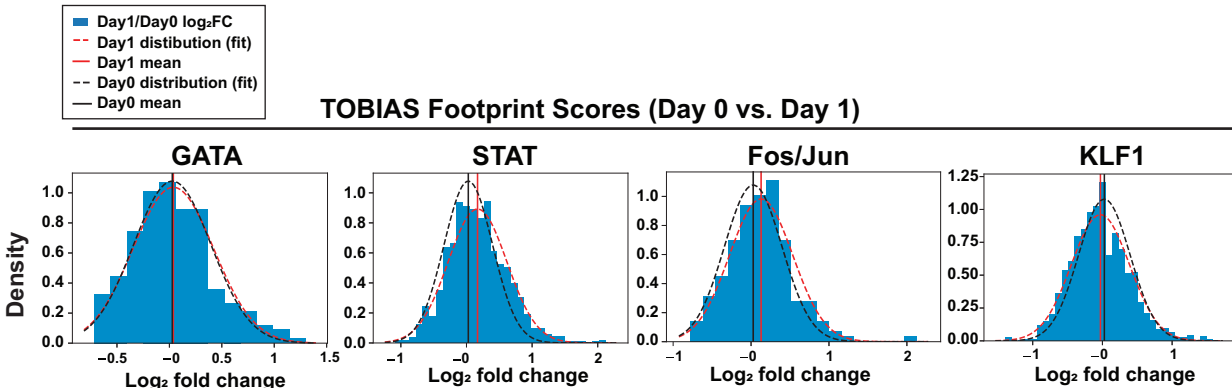
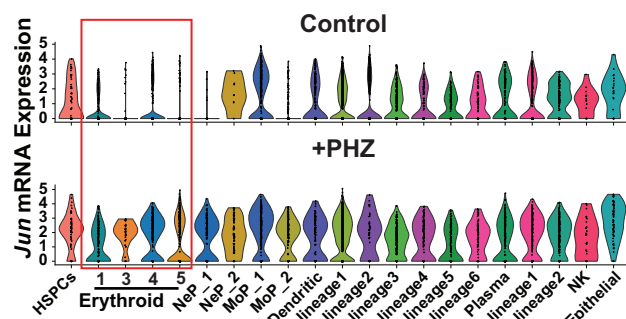
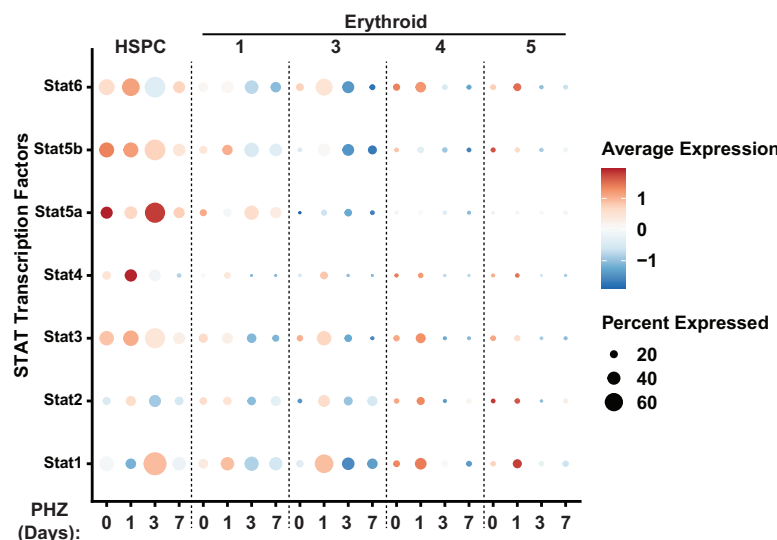
43

44

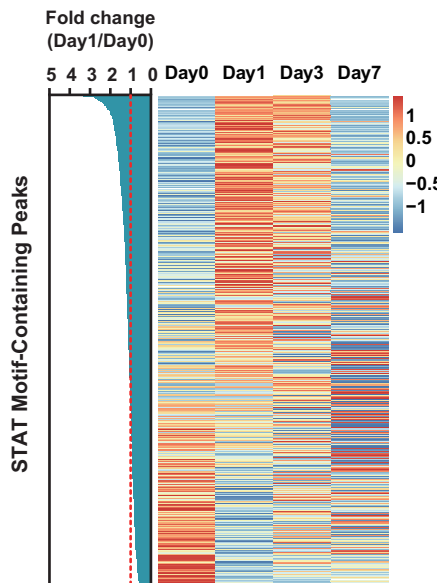
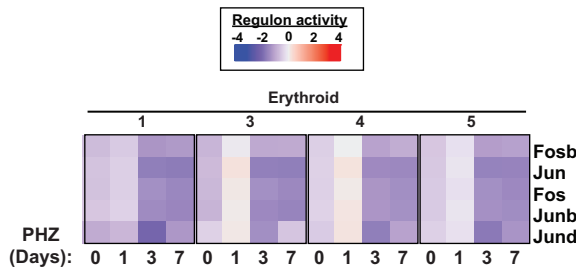
45

46

47

A**B****C****D**

STAT (STAT5a::STAT5b_MA0519.2) TOBIAS Footprint Scores

**E**

48 **SUPPLEMENTAL FIGURE LEGENDS**

49

50 **Supplemental Figure 1. Early onset changes to chromatin post-anemia in erythroid cells**
51 **are associated with increased AP-1 footprint, gene expression, and activity scores.** A)
52 Density plots represent a HOMER motif analysis at regions where ATAC-seq peaks were
53 gained 24 hours post-PHZ. TF motifs corresponding to ATAC footprinting (TOBIAS) analysis:
54 GATA1 (MA0035.5), Stat5a/Stat5b (MA0519.2), Fos/Jun (MA1126.2), and KLF1 (MA0493.3).
55 B) Jun mRNA expression plots from single cell RNA-seq progenitor data (all Kit⁺ cells)
56 annotated as HSPCs, erythroid clusters, neutrophils (NeP), monocytes (MoP), Dendritic, B
57 cells, T cells, Natural Killer (NK) plasma and epithelial cells. Units of expression are relative
58 log normalized. Error bars represent SD. ***p<0.001 (Wilcoxon signed rank test). C) Dot plot
59 depicting single cell RNA-seq analysis of HSPC and erythroid-specific expression of all
60 detectable components of the AP-1 transcription factor family at 0, 1, 3, and 7 days post-PHZ.
61 D) Heat map of genomic regions containing Stat5a/5b motifs (MA0519.2) with changes to
62 TOBIAS footprint scores between 0- and 1-day post-PHZ, ranked by fold change. E) SCENIC
63 analysis comparing the regulon activity of AP-1 components in erythroid cells at 0, 1, 3, and 7
64 days post-PHZ.

65

66

67

68

69

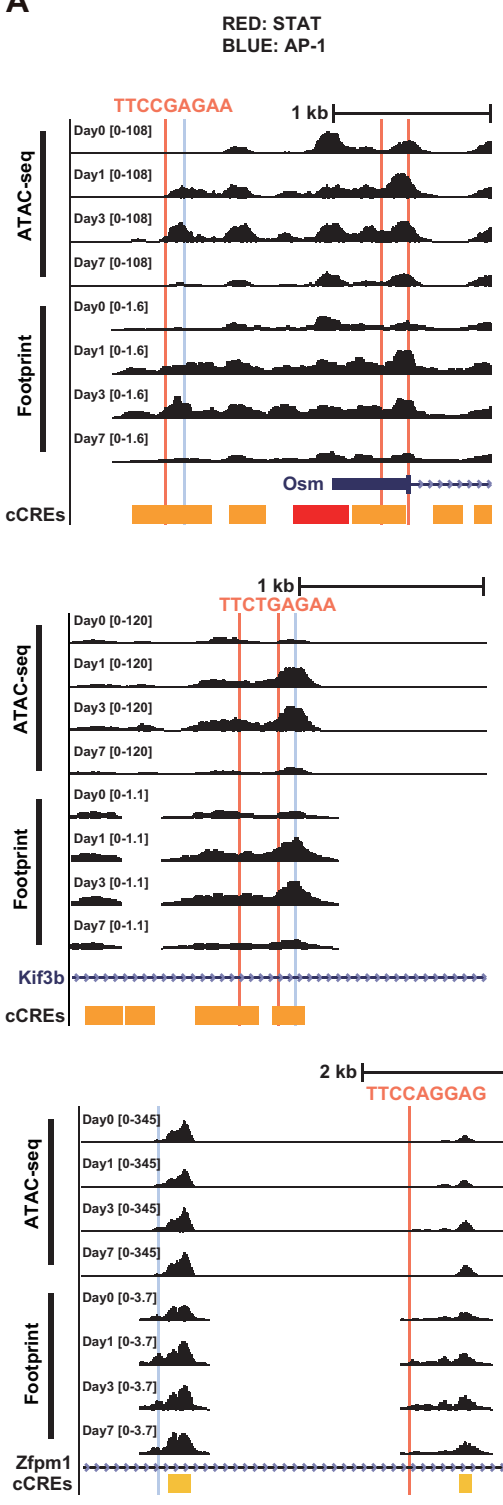
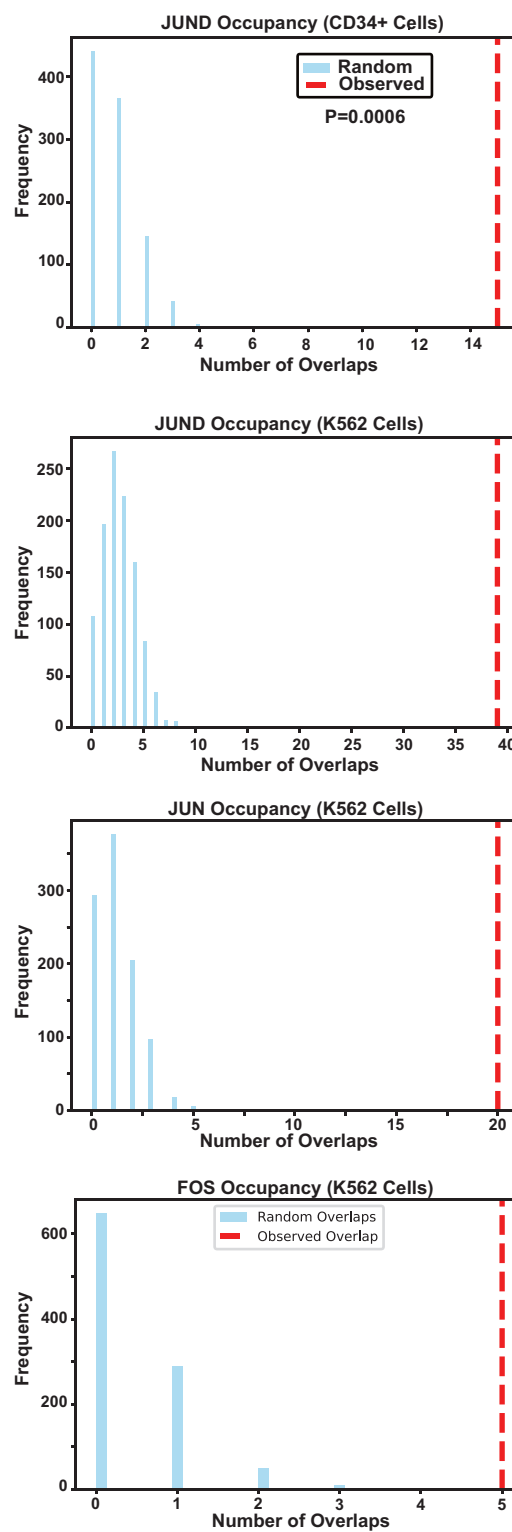
70

71

72

73

74

A**B**

75 **Supplemental Figure 2. Anemia recovery alters ATAC footprints at sites associated with**
76 **signal-responsive AP-1 and STAT sites and known AP-1 occupancy sites.** (A) ATAC-seq
77 and TOBIAS Footprint scores at the *Osm*, *Kif3b*, and *Zfpm1* loci. Blue line demarcates region
78 with changing AP-1 footprint score. Red line demarcates region with changing STAT footprint
79 score. cCREs were classified by ENCODE. Red=promoter, orange=proximal enhancer-like
80 signature. (B) Plots depict the overlap in ChIP-seq observed (dotted red line) and random
81 (blue lines) occupancy of JUND (CD34+), JUND (K562), JUN (K562), and FOS (K562) at 178
82 sites with AP-1 footprints changing at day 1 post-PHZ. Blue lines were calculated by randomly
83 assigning 178 ATAC-seq peaks and comparing against ChIP-seq data.

84

85

86

87

88

89

90

91

92

93

94

95

96

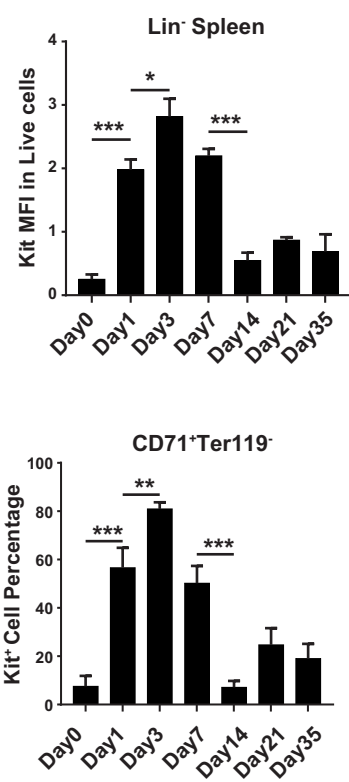
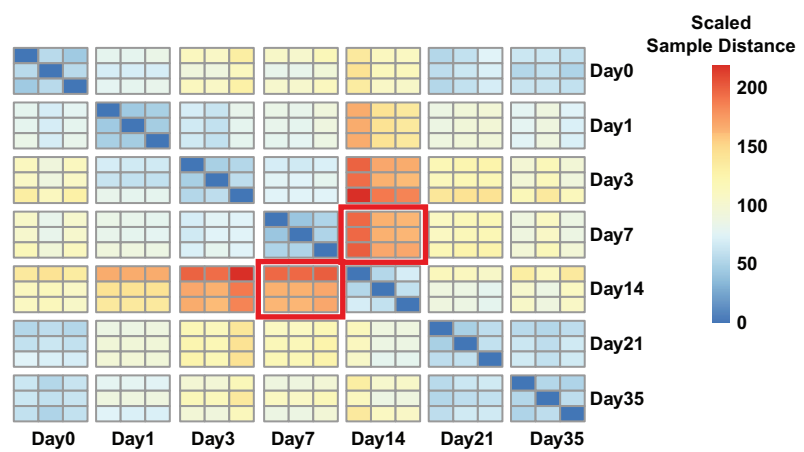
97

98

99

100

101

A**B**

102 **Supplemental Figure 3. Changes in the frequency of Kit+ and erythroid precursors at**
103 **time points post-PHZ and chromatin occupancy.** A) (top) Flow cytometry analysis of the
104 Kit median fluorescence intensity (MFI) in live (DAPI-negative) Lineage-negative spleen cells.
105 (bottom) Flow cytometry analysis of the percentage of Kit-positive cells in live (DAPI-negative)
106 Lineage-negative CD71-positive, Ter119-negative spleen cells. B) Scaled sample distance
107 depicting ATAC-seq comparisons of individual replicates between each time point post-PHZ
108 (days 0, 1, 3, 7, 14, 21, and 35 (N=3). Statistical significance was determined by two-tailed
109 unpaired Student's t test. *p<0.05, **p<0.01, ***p<0.001.

110

111

112

113

114

115

116

117

118

119

120

121

122

123

124

125

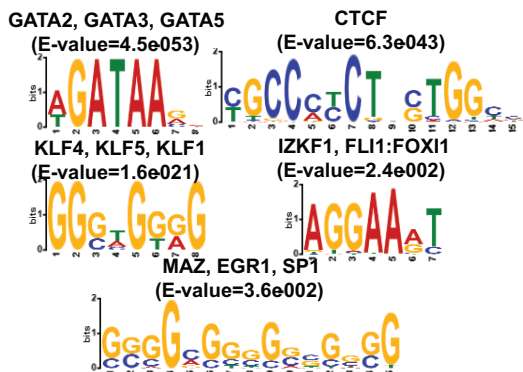
126

127

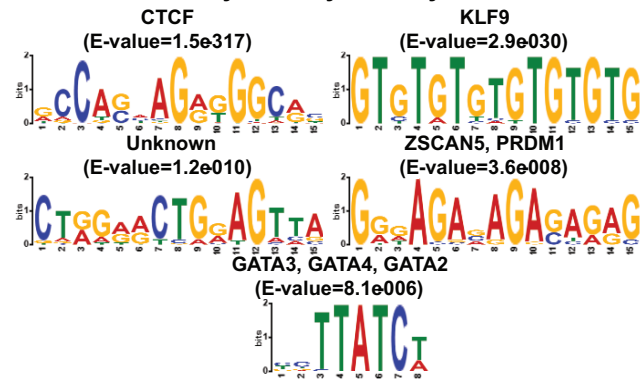
128

A

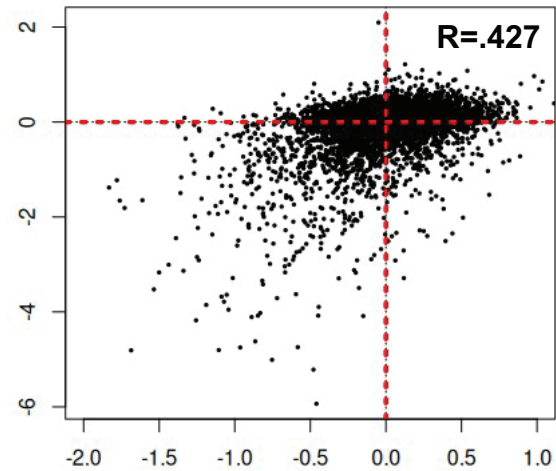
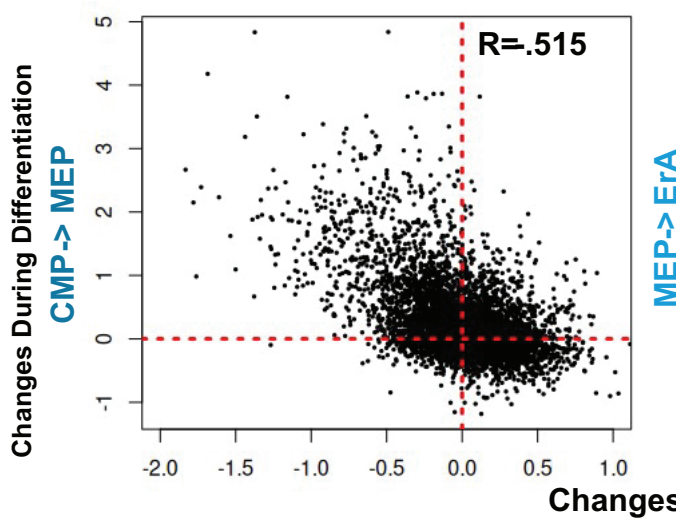
acute peaks n=6065
(Day0 vs Day7)



long lasting peaks n=893
Day0 vs Day7 vs Day35



B



129 **Supplemental Figure 4. Assigning temporal and durable chromatin changes in acute**
130 **anemia to discrete functional cell types.** A) Motif analysis (MEME-ChIP) at regions where
131 ATAC-seq peaks were transiently gained or lost at 7 days post-PHZ, followed by restoration
132 of the original state, and at regions where ATAC-peaks remained durably elevated at 35 days
133 post-PHZ. B) Comparisons of PHZ-induced chromatin changes to chromatin changes which
134 occur during transitions between common myeloid progenitor (CMP), megakaryocyte-
135 erythrocyte progenitor (MEP), and committed erythroid precursors (EryA).

136

137

138

139

140

141

142

143

144

145

146

147

148

149

150

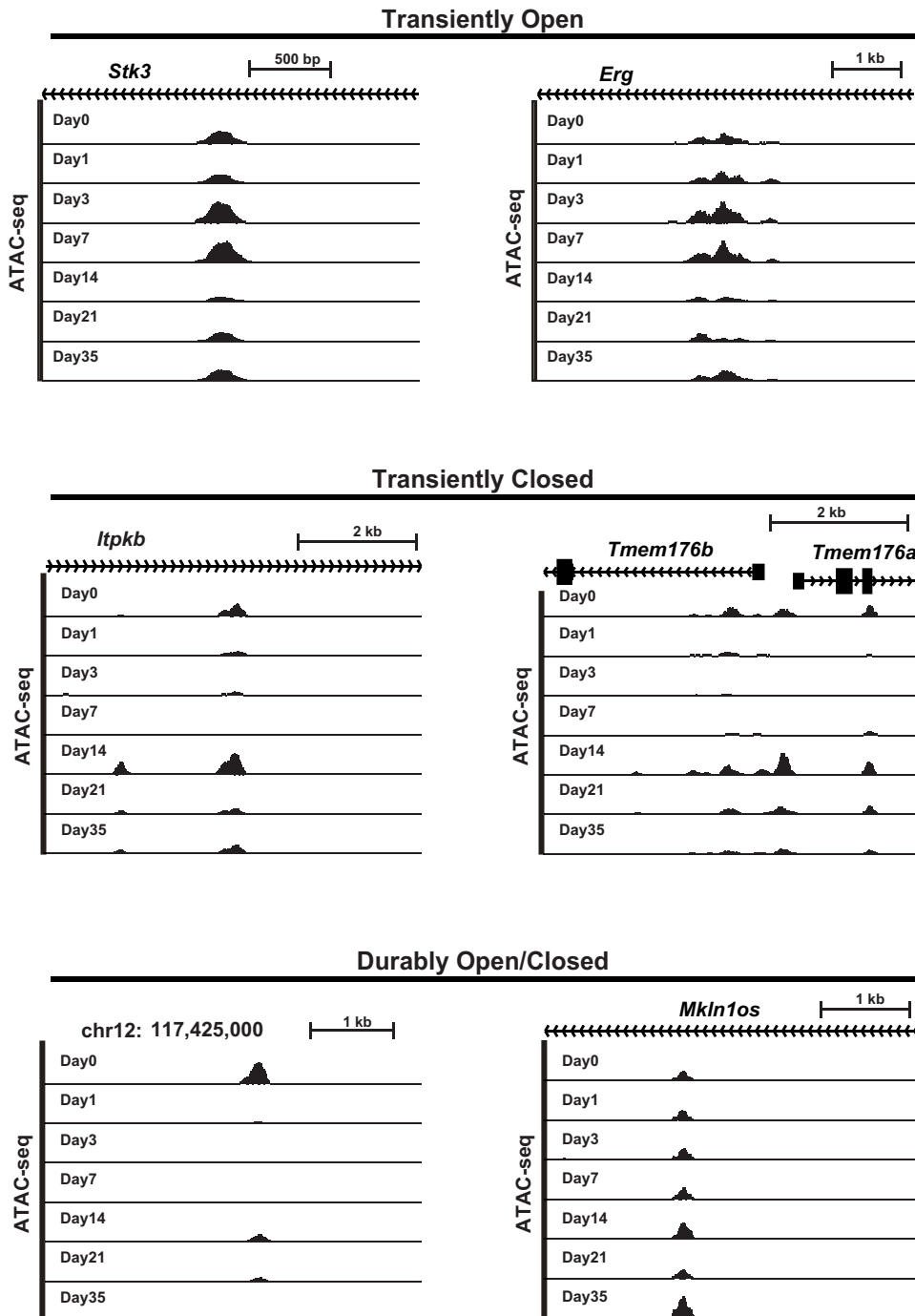
151

152

153

154

155



156 **Supplemental Figure 5. Transient and durable changes to chromatin accessibility over**
157 **a 35-day anemia-recovery time course.** UCSC genome browser tracks depict examples of
158 ATAC-seq data from transiently open, transiently-closed and durably changed chromatin
159 accessible regions.

160

161

162

163

164

165

166

167

168

169

170

171

172

173

174

175

176

177

178

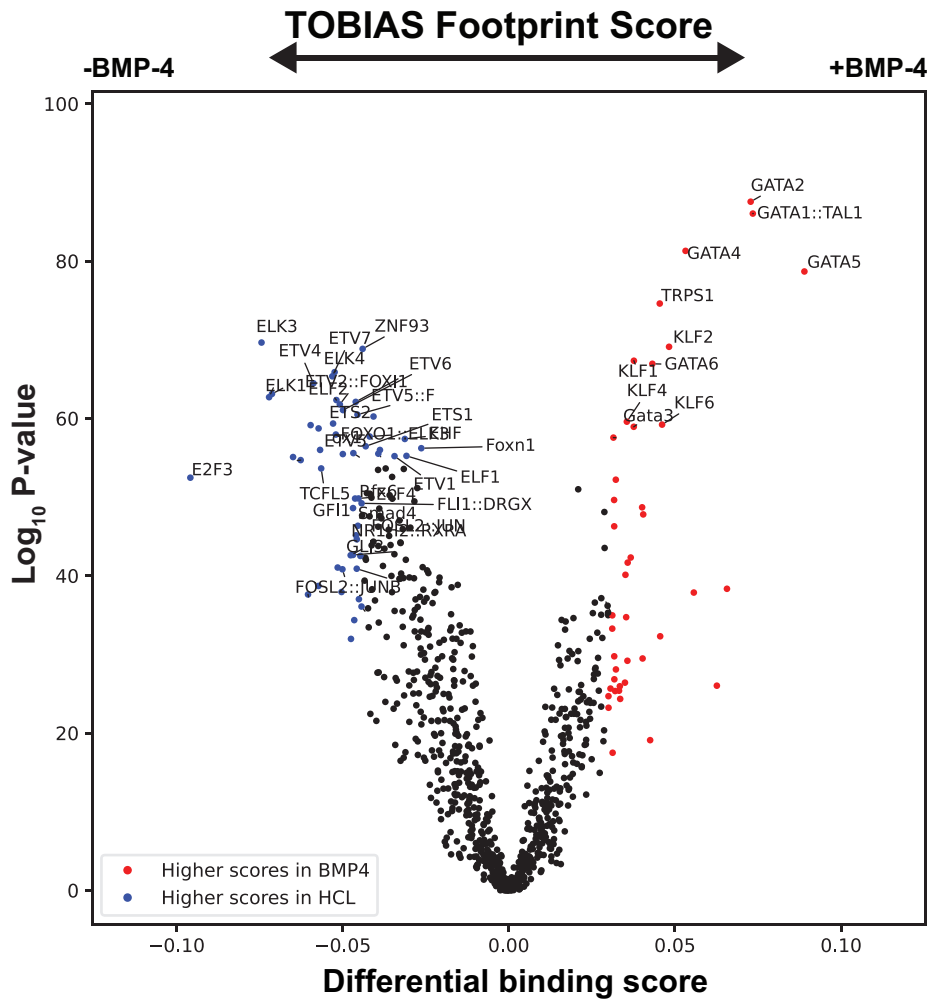
179

180

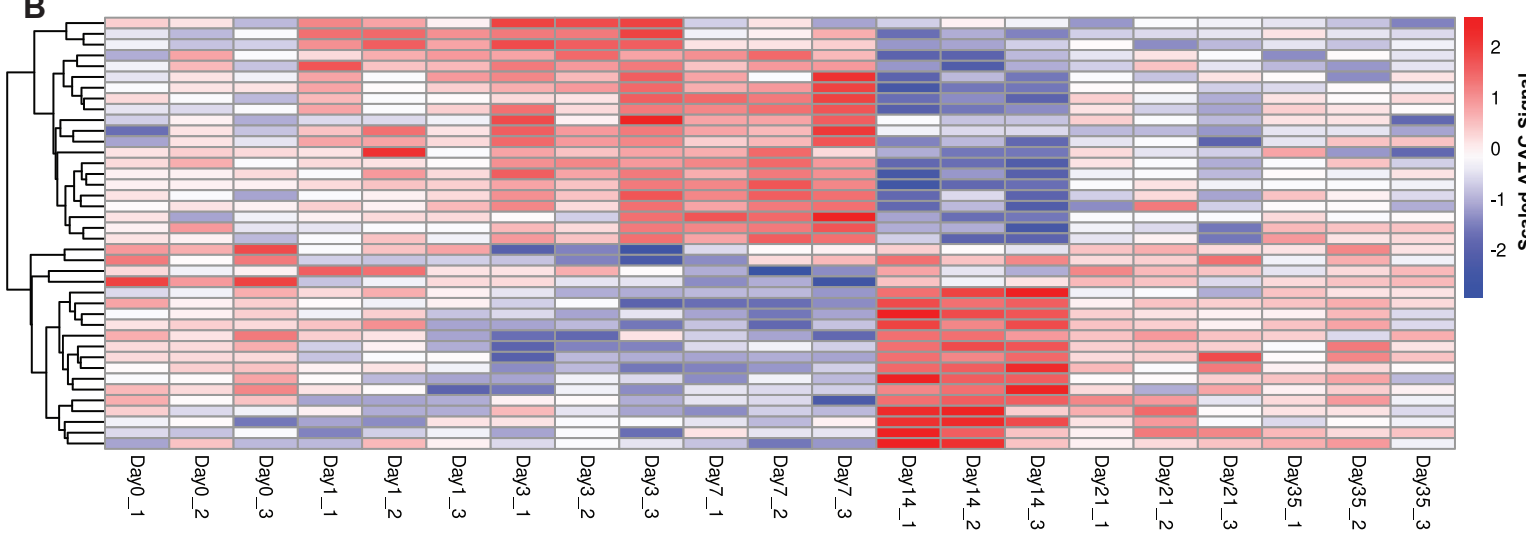
181

182

A



B



183 **Supplemental Figure 6. BMP-4 induces chromatin accessibility changes at select sites**
184 **genome wide.** A) Volcano plot of transcription factor motif differential binding scores in control
185 vs. BMP-4-stimulated human primary erythroid cultures on the x-axis (calculated using
186 TOBIAS) and -log10 (p value) on the y-axis. Each dot represents one transcription factor
187 assigned by consensus motif. B) Heat map depicts the ATAC signal (scaled based on each
188 regions max signal) of 39 chromatin sites which are BMP4-sensitive and either activated or
189 repressed in acute anemia induced by PHZ.

190

191

192

193

194

195

196

197

198

199

200

201

202

203

204

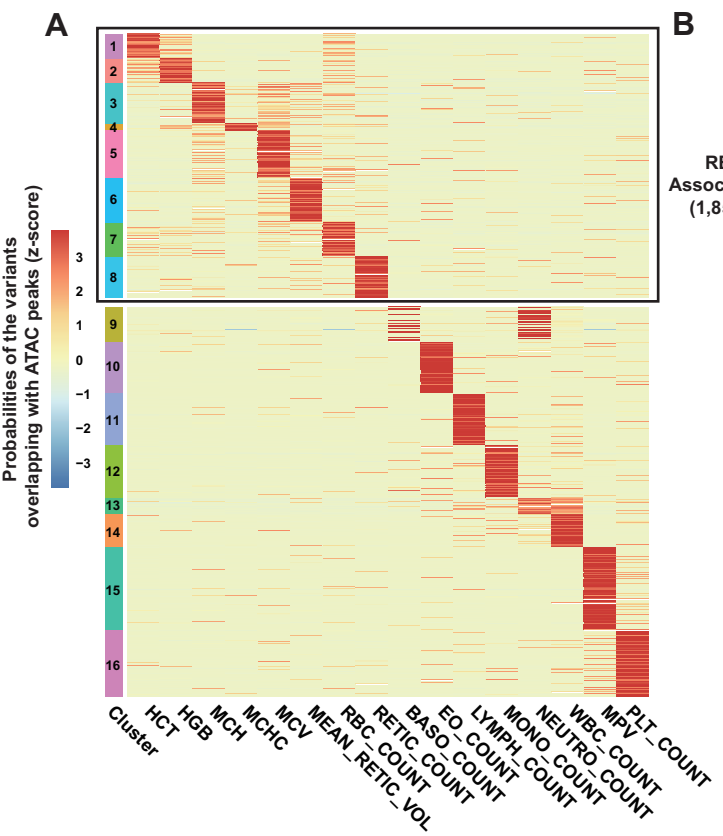
205

206

207

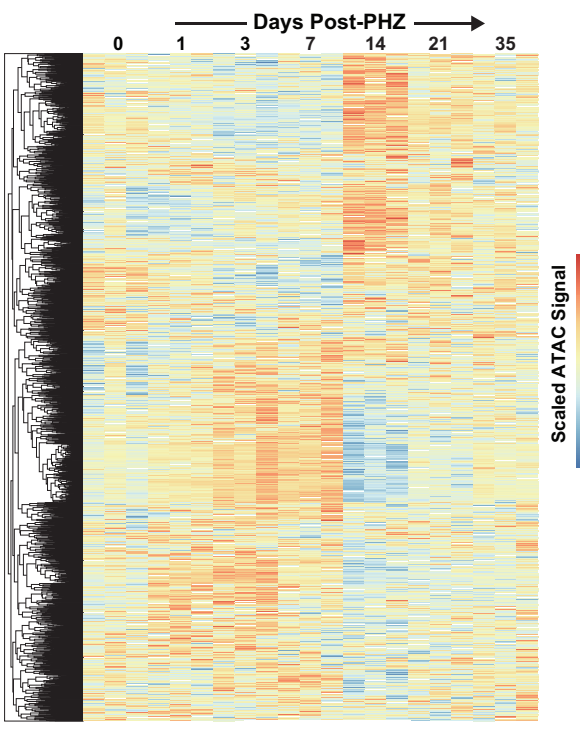
208

209



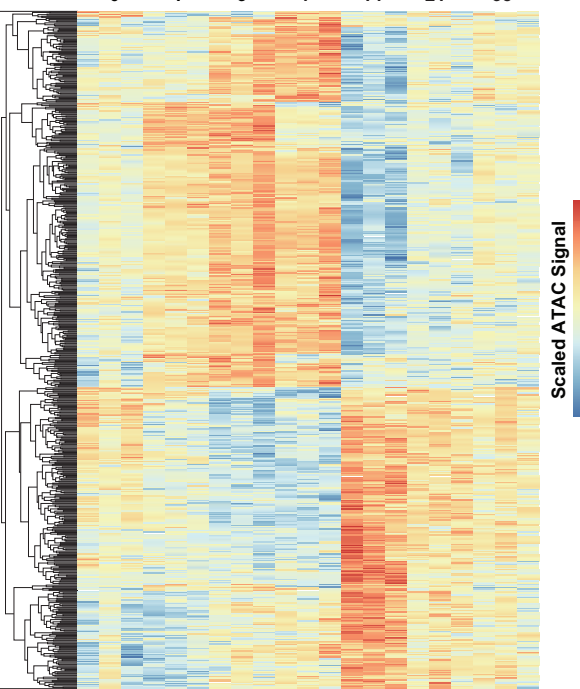
B

RBC Trait-Associated Peaks (1,857 peaks)



C

RBC Trait-Associated Significantly Changed Peaks (618 peaks)



210 **Supplemental Figure 7. Evaluating SNPs linked to hematologic traits at anemia-**
211 **sensitive cis-elements.** A) After human (hg38) to mouse (mm10) lift-over, heat map depicts
212 the probability that individual SNP variants overlap with peaks in the mouse genome. B) Heat
213 map of scaled ATAC-seq signal at each of the trait-associated SNPs. C) Heat map of scaled
214 ATAC-seq signal at SNPs associated with red blood cell traits.

215

216

217

218

219

220

221

222

223

224

225

226

227

228

229

230

231

232

233

234

235

236

237

238 **SUPPLEMENTAL REFERENCES**

239 1. Bailey, T.L., Johnson, J., Grant, C.E. and Noble, W.S. (2015) The MEME Suite. *Nucleic*
240 *Acids Res*, **43**, W39-49.

241 2. Shao, Z., Zhang, Y., Yuan, G.C., Orkin, S.H. and Waxman, D.J. (2012) MAnorm: a
242 robust model for quantitative comparison of ChIP-Seq data sets. *Genome Biol*, **13**,
243 R16.

244 3. Langmead, B. and Salzberg, S.L. (2012) Fast gapped-read alignment with Bowtie 2.
245 *Nat Methods*, **9**, 357-359.

246 4. Danecek, P., Bonfield, J.K., Liddle, J., Marshall, J., Ohan, V., Pollard, M.O., Whitwam,
247 A., Keane, T., McCarthy, S.A., Davies, R.M. *et al.* (2021) Twelve years of SAMtools
248 and BCFtools. *Gigascience*, **10**.

249 5. @misc{Picard2019toolkit, title = {Picard toolkit}, year = {2019}, publisher = {Broad
250 Institute}, journal = {Broad Institute, G.r., {\url{https://broadinstitute.github.io/picard/}}},
251 h. and }.

252 6. Ramirez, F., Dundar, F., Diehl, S., Gruning, B.A. and Manke, T. (2014) deepTools: a
253 flexible platform for exploring deep-sequencing data. *Nucleic Acids Res*, **42**, W187-
254 191.

255